Double network hydrogel sensors with high sensitivity in large strain range

Jingfei Zhang[1], Wei Xue[2], Yongqiang Dai[1], Lian Wu[1], Bing Liao[1*], Wei Zeng[1*], Xiaoming Tao[3]

1. Guangdong Provincial Key Laboratory of industrial surfactant, Institute of Chemical Engineering, Guangdong Academy of Sciences, Guangzhou 510665, China

2. Department of Biomedical Engineering, Jinan University, Guangzhou 510632, China

3. Research Centre for Smart Wearable Systems, Institute of Textiles and Clothing, The Hong Kong Polytechnic University, Hong Kong

E-mail: liaobing@gic.ac.cn; zengwei@gdcri.com

ABSTRACT

Owing to their preferable flexibility and facilitation to integrate with various apparel products, flexible sensors with high sensitivity are highly favored in the fields of environmental monitoring, health diagnosis, and wearable electronics. However, great challenges still remain in integrating high sensitivity with wide sensing range in one single flexible strain sensor. Herein, a new stretchable conductive gel-based sensor exhibiting remarkable properties regarding stretchability and sensitivity is developed via improving the ionic conductivity of the PVA/P(AM-AANa) double network hydrogel. Specifically, the strain sensor developed exhibits an excellent elongation of 549%, good fatigue resistance and recovery performance. Simultaneously, the hydrogel strain sensor shows a high conductivity of 25 $mS \cdot cm^{-1}$, fast response time of 360 ms, and a linear response (gauge factor =4.75) to external strain (≈400%), which endow the sensor with accurate and reliable capacities to detect various human movements. Integrating the merits of flexibility, environment friendliness, and high sensitivity, the conductive gel-based sensor has promising application prospects in human-machine interfaces, touchpads, biosensors, electronic skin, wearable electronic devices and so on.

KEYWORDS

Strain Sensor, Double Network Hydrogel, High Mechanical Properties, Flexible, High Sensitivity

1. Introduction

Wearable strain sensors are essential for realizing the application of sensor devices in people's work and life, such as smart home, health monitoring, biological engineering, etc.[1-5] Ideal wearable strain sensors should attach to human skin comfortably, and monitor human motions with a broad sensing range, high accuracy, and excellent durability. In addition, sensors must also meet the requirements of flexibility, low power consumption, biocompatibility, portability, compatibility with the human body.[6-9] Conventional semiconductors-based strain sensors fail to meet some of the above requirements due to their intrinsic brittle and rigid nature. Therefore, significant efforts have been devoted in designing novel sensors, among which the combination of intrinsically conductive filler and stretchable polymer is considered to be a preferable strategy for developing highly sensitive and stretchable sensors.

Typically, electronic-conductive flexible sensors are prepared by embedding MXene fillers[10-13], metal nanomaterials (nanoparticles, nanowires), conductive carbon nanomaterials (carbon nanotubes, graphene oxide)[14] and intrinsically conductive polymers (polypyrrole,[15, 16] polyaniline,[17] and poly(3,4-ethylenedioxythiophene): poly(styrene-sulfonate)[18]) in the polymer film or elastic matrix.[19-21] Recently, Luo synthesized silver nanowire-acrylate composite to achieve the gauge factor value as high as 10486, yet the maximum stretchability was below 20% strain.[20] Applying a similar strategy, Chen et al. integrated pristine multi-walled carbon nanotubes (MWNTs) into gelatin hydrogel, the resulting sensor exhibited a gauge factor of 0.99 in the range

of 100% strain.[22] Du and coworkers developed conductive hydrogels composed of polyvinyl alcohol (PVA) and PEDOT:PSS, achieving a gauge factor of 4.4 (100% strain).[23] Despite the tremendous progress made in this burgeoning field, the application of these electronic-conductive flexible sensors in wearable devices is still hindered by the low fraction strain as a result of the uneven distribution of conductive fillers and the Young's modulus mismatch between the rigid conductive component and the flexible matrix.[24]

In the search for alternatives, ion-conductive hydrogels have been identified as promising candidates for the development of flexible sensors with large strain range and high sensitivity. With their unique porous structure, ion-conductive hydrogels can provide effective channels for ion transportation,[25, 26] i.e., high ionic conductivity. Meanwhile, they are highly flexible and transparent with good biodegradability and biocompatibility,[27-29] which resolves the issue of low fracture strain associated with the conventional conductive materials.[30, 31] The superiority of ion-conductive hydrogels has been proven by relevant studies. For example, Sui et al. fabricated ionic strain sensors based on agar/polyacrylamide double network hydrogels with sodium chloride as conductive ions, and the sensors exhibited a good conductivity of 0.04 $S \cdot m^{-1}$ and a gauge factor of 2.1 at strain of 1600%.[32] Lai synthesized a highly stretchable hydrogel consisting of lithium chloride, polyacrylamide and sodium carboxymethylcellulose, showing a gauge factor of 3.15 at strain of 1200%.[33]

In general, chemically cross-linked hydrogels have good mechanical properties. However, these properties will degrade significantly in subsequent experimental tests

as the irreversible breakage of covalent bond during the deformation process causes permanent deformation. In comparison, physically cross-linked hydrogels constructed by non-covalent interactions can be restored after deformation, and therefore have better tensile properties and self-healing ability.[34, 35] In recent studies on hydrogel sensors, single-network hydrogels typically exhibit unsatisfactory mechanical properties,[36] while good rigidity and toughness have been achieved by the double network (DN) hydrogels obtained by cross-linking of hard and brittle polyelectrolyte networks and soft neutral polymerization. Moreover, DN hydrogels have been proven to improve the sensing performance and mechanical properties of sensors simultaneously.[37]

Herein, we demonstrate an ionic-conductive DN hydrogel-based wearable strain sensor with high sensitivity and a large strain range. The DN hydrogel was fabricated by the interpenetration of the first network formed by the free-radical polymerization of acrylamide (AM) and sodium acrylate (AANa) and the second network formed by the crystal regions of PVA chains. Sodium chloride was added in the hydrogel system to improve the conductivity of the hydrogel through ion transportation in the porous networks. The mechanical performance can be improved through the hydrogen bonding interaction and microcrystalline structure, therefore, the DN hydrogels can dissipate a lot of energy during stretching process to ensure high ductility and high elasticity, achieving the stable sensing performance. Interestingly, the hydrogel sensor exhibits high sensitivity in the entire strain interval, reliable repeatable performance up to 1300 cycles and fast response time of 360 ms. The resulting hydrogels have promising

application prospects in wearable sensors due to their simplicity in preparation process, high stretchability, excellent recoverability and high gauge factor.

2. Results and discussion

2.1. Fabrication and Characterization of the DN hydrogels

The ion-conductive DN hydrogels were fabricated using PVA, AM and AANa via a simple two-step approach, i.e., free radical in situ polymerizations and freeze-thaw treatment in the presence of NaCl, as shown in **Figure 1**(a). Firstly, the chemically cross-linked P(AM-AANa) network was formed through free radical polymerization as the first network and are the main driving force for hydrogel formation. Afterwards, through the cyclic freeze-thaw treatment, the PVA molecular chains formed the microcrystalline structure and hydrogen bonds,[38-40] which were physical crosslinking points, connecting PVA chains with the first chemical network to form a double network (Figure S1(a) and S1(c)). In order to reveal the formation of DN hydrogels, FT-IR measurements were carried out and the spectra are in Figure 1(b). It can be seen that the peak at 1653 cm^{-1} is caused by the stretching vibration of the carbonyl group (-C=O) in the carboxyl and amide functional groups. Besides, the peaks at 1610 cm^{-1} and 1280 cm^{-1} in the FT-IR spectra of the AM respectively generated by the stretching vibration absorption of C=C and the flexural vibration absorption of C-H of the C=C bond. The peaks associated with C=C bond disappeared in the FT-IR spectrum of the DN hydrogel, indicating the formation of covalent crosslink between AM and AANa through polymerization. In addition, the strong and broad peaks at 3300 cm^{-1} and 3324 cm^{-1} are

respectively caused by the stretching vibration of -OH groups in PVA and PAANa, while the corresponding -OH peak shifted to 3330 cm^{-1} in the DN hydrogel. The peak at 1142 cm^{-1} generated by the stretching vibration of C-O in the PVA crystal region disappeared in the FT-IR spectra of the DN hydrogel. Besides, the absorption peak at 3227 cm^{-1} generated by symmetric stretching vibration of PAM shift to 3187 cm^{-1} in the hydrogel. These above results indicate that cyclic freeze-thaw treatments promoted the formation of the intermolecular or intramolecular hydrogen bond in the hydrogel, as well as the physical cross-links in the crystalline region. In addition, the SEM micrograph of DN hydrogel (Figure 1(c)) suggests a uniform distribution of porous structure. The porous structure provides the hydrogels with rapid recovery ability and excellent stretching performance.

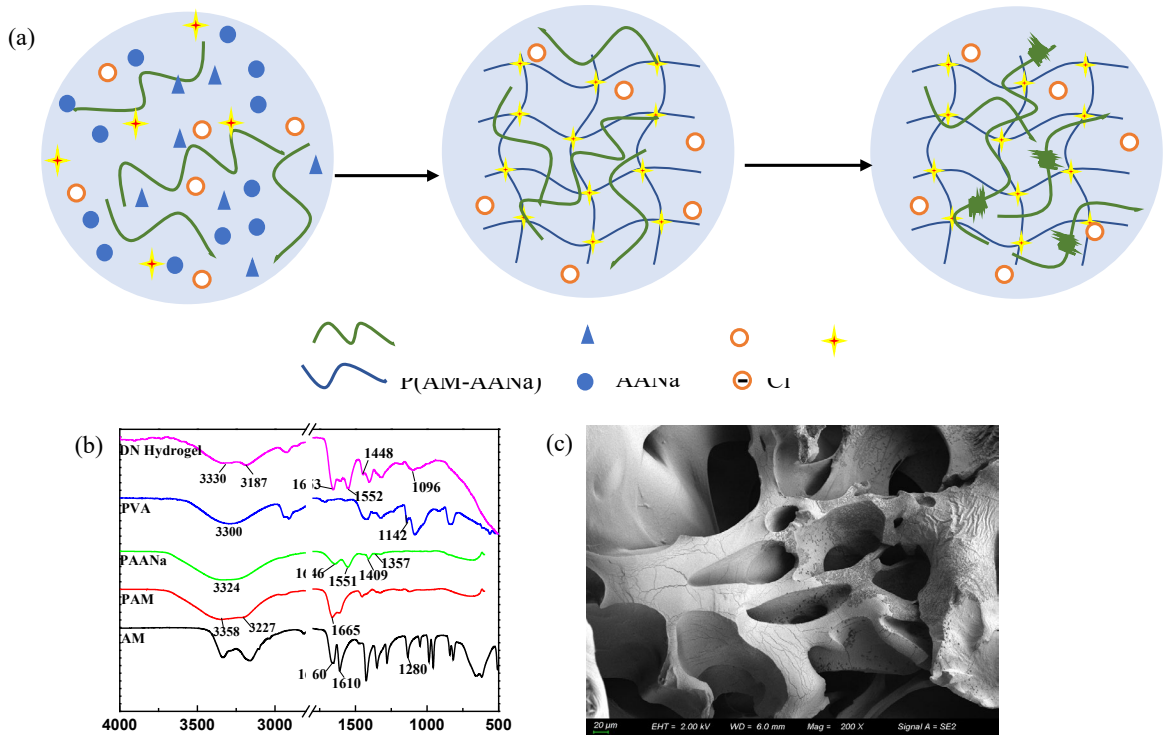

Figure 1. (a) A schematic diagram of the preparation of PVA/P(AM-AANa) ion-conductive DN hydrogels. (b) FT-IR spectra of DN hydrogels. (c)The SEM of freeze-dried DN hydrogel.

2.2. Sensing performance of the ion-conductive DN hydrogels

NaCl was introduced into the DN hydrogel to improve the ionic-conductivity. With a NaCl content of 1.0 wt%, the hydrogel exhibited a conductivity of 25 $mS \cdot cm^{-1}$, which is considerably higher than that of the pure DN hydrogel (2.08 $mS \cdot cm^{-1}$) (Figure S1(e)). The conductivity value is superior to that of some hydrogel sensors reported (e.g., 0.4,[32] 0.57,[41] 7.6,[30] and 16.2 $mS \cdot cm^{-1}$[42]), which could be attributed to the construction of the three-dimensional (3D) ion transport channels and the efficient facilitation of ion diffusion. Increasing content of NaCl up to 3.0 wt%, while the improvement the hydrogel conductivity was not significantly (Figure S1(e)), the tensile strength gradually increases from 189 kPa to 230 kPa and the break elongation decreased from 630% to 494% (Figure S1(b) and Figure S1(d)). Besides, the results of rheological properties indicate the stability and excellent elastic properties of the 3D network hydrogel structure throughout the test range (Figure S2). The hydrogel containing 1.0 w% NaCl was selected as the optimized sample for significantly improving the conductivity without causing an obvious degradation of mechanical properties. The break elongation and the tensile strength of the optimized sample were respectively 549% and 223 kPa.

Further, in order to investigate the sensing behaviors of the ion-conductive hydrogel sensor, the gauge factor (GF, $GF= \Delta R/ (R_0 * \varepsilon)$) was used to evaluate its sensitivity. As shown in **Figure 2**(a), the sensitivity in various strain intervals were calculated respectively and a good linear response was observed in each strain interval. Here, large strains produce more significant changes in the conductive path and more

pronounced changes in relative resistance, resulting in larger $\Delta R/R_0$ values.[18, 36, 43] It is notable that the GF is 2.58 in the strain range of 100%. Moreover, in the large strain range (300% ~ 400%), the GF value rose rapidly with a highly linear relationship (R^2 = 0.9998) and reached 4.75. In fact, as shown in Figure 2(b) and Figure S5, the data displayed a highly linear relationship (R^2 =0.9899) over the entire strain interval with a GF value of 3.81, which is higher than most hydrogel-based strain sensors reported in literature (GF = 1.51,[44] 0.63,[43] 0.84,[45] 0.478,[25] 1.32,[46] 1.54,[29] 1.58[18]).

Further response time test was performed for the hydrogel sensor under instantaneous tensile deformation to reveal the response behavior. Specifically, the response time of the hydrogel sensor was 360 ms when 1% strain was applied (Figure 2 (c)). The high sensitivity and rapid response features of the hydrogel sensor are beneficial for potential applications in real-time monitoring of human physiological signals.

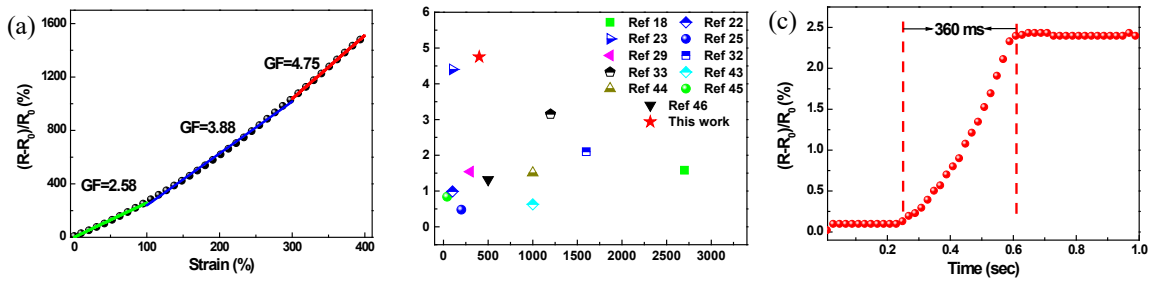

Figure 2. (a) Response value of hydrogels at various tensile strains. (b) Comparison of the sensitivity and sensing range of the sensor with other previously reported strain sensors. (c) Response time of hydrogel sensor under instantaneous tensile deformation.

The sensing performances of the DN hydrogel are presented in **Figure** 3. The response values of the ion-conductive hydrogel sensor show a steady waveform

consistent with the strain of 100% during the ten loading-unloading cycles, and remain essentially constant at the same strain (Figure 3(a)). Meanwhile, as shown in Figure 3(b), in the strain range of 10%-100%, the same change trend was observed for the response values at different strains and the stable value was found to be dependent on the strain. No obvious decay of sensing performance was observed during the test. These results indicate a high repeatability, stability and excellent sensitivity of hydrogel sensor. Its superior performance is owing to the hydrogen bond between the two networks acts as a "sacrificial bond" to resist external effects. With this mechanism, the hydrogel can still be restored to its original shape and display good recovery performance (Figure S1(f)).

To gain in-depth understanding of the ion-conductive hydrogel sensor's sensing behaviors, the sensing performances were tested applying strains from 0% to 60% in increments of 10% and from 0% to 200% in increments of 50%, with a dwell time of 10 s at each step followed by a gradual return to 0%. As shown in Figure 3(c), the response value of the sensor increases step-by-step with the increasing tensile strain and the value is basically stable under a fixed strain. Moreover, due to the remarkable elasticity of the hydrogels, the response value can basically recover along with the strain recovery process, demonstrating high sensitivity and stability of the sensor.

Figure 3(d) further shows the response value of the sensor under various cyclic strains. At a tensile strain of 75%, 150%, 200% and 250%, the response value is 180%, 360%, 560% and 780%, respectively. Moreover, the current signal exhibits repeatable and reliable changes during the five loading-unloading cycles, indicating excellent

reversibility and fast response of the hydrogel sensor. In addition, the compressive sensing performances of the DN hydrogels were tested and the results are presented in Figure 3(e) and 3(f). Similarly, as reflected by the relative resistance changes observed over 10 cycles at a compressive strain of 40% and under cyclic compressive strains from 10% to 60% (held for 5 s at every different strain), high sensitivity and stability of sensor was also confirmed.

It is a general tendency that the value of $\Delta R/R_0$ rises significantly as the applied strain increases and then completely returns to the initial value upon removing the strain, indicating a remarkable strain-induced stability and reversibility. The superior property of the sensor is related to the sensing mechanism of the ion-conductive DN hydrogel, i.e., the variations of ions concentration in hydrogel during the tensile or compressive cycles of the sensor (Figure 3(g)). Specifically, the conductivity of hydrogel mainly depends on the directional movement of anions and cations in the porous network of the hydrogel. A larger strain means longer distances between ions, i.e., decreased number of movable ions (Na^+ and Cl^-) per unit length. This results in a change in resistance. Besides, since DN hydrogels are highly resilient, the distances between ions are restored to the initial state during the recovery process, causing the conduction path to recover.

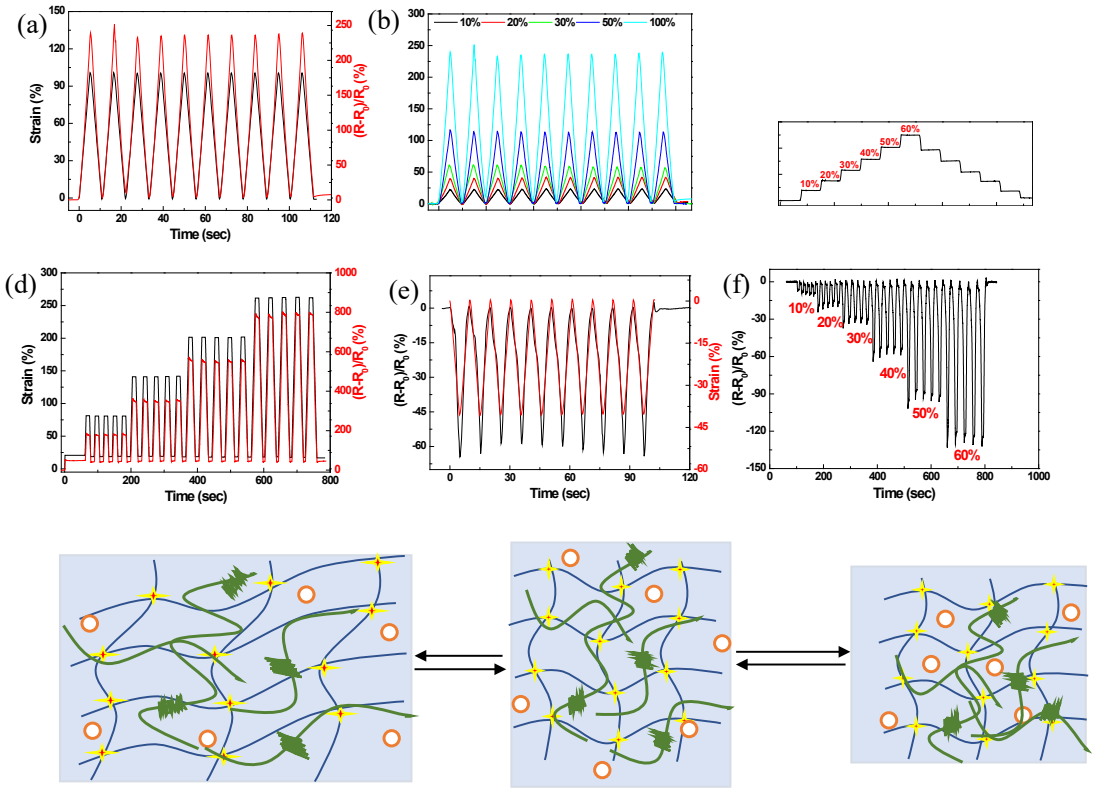

Figure 3. Sensing performances of the hydrogel under conditions of (a) Periodical tensile strain of 100% (black) vs time and the corresponding response value (red). (b) various strains ranging from 10% to 100% (10 cycles each strain). (c) Tensile strain from 0% to 60% and from 0% to 200%, (held for 10 s at each strain). (d) various tensile strain cycles (75%, 150%, 200%, 250%). (e) periodical compressive strain of 40% and (f) Compressive strain from 10% to 60%, held for 5 s at each strain. (g) Schematic diagram on the change of ion concentration in hydrogel with tensile and compressive strains.

To acquire the dynamic response behaviors of the DN hydrogel sensor, a constant strain of 40% was applied at various stretching speeds (50 mm/min ~ 500 mm/min) and the response values of the hydrogel sensor were recorded, as shown in **Figure 4**(a). The response value is basically stable at a fixed stretching rate and increases slightly at higher stretching rate, which is attributed to the recovery delay and slight slippage of

the hydrogel.[33] Besides, even at high stretching speed (500 mm/min), a durable and steady response signal was acquired, indicating the satisfactory performance of the hydrogel sensors at both high or low stretching rates. The results imply that the hydrogel sensors can be well adapted to a wide range operating frequency. Furthermore, as presented in Figure 4(b), the response signal of the DN hydrogel sensor is stable regardless of the voltage (0.5 V~3 V) applied. More importantly, the sensors can still generate effective and stable electrical signals at an extremely low voltage of 0.5 V, suggesting the high strain-sensitivity of the hydrogel is independent of the applied voltage. Such a low voltage working environment of the hydrogel sensor is very suitable for the preparation of portable sensors, which can be applied to lightweight wearable devices. Besides, a constant strain of 10% was applied to the strain sensor and kept for 100 minutes to observe the drift characteristics of the sensor under static loading. More importantly, the response value of the strain sensor remained almost constant throughout the whole process (Figure 4(c)), indicating a remarkable static strain induction stability.

For evaluating the repeatability and durability of the hydrogel sensor in practical application, a continuous loading-unloading test was carried out at a strain of 5% (1300 cycles). As shown in Figure 4(d), it is worth noting that $\Delta R/R_0$ is identical in each cycle and shows a stable response during the 1300 tensile loading-unloading cycles, demonstrating the excellent stability and reproducibility of the hydrogel sensor in the long-term loading-unloading process. In addition, as shown in Figure S6, a continuous loading-unloading measurement at a large strain of 80% was also carried out. The

response was also observed to remain steadily throughout 500 loading-unloading cycles, indicating the excellent stability of the sensor even under a large strain.

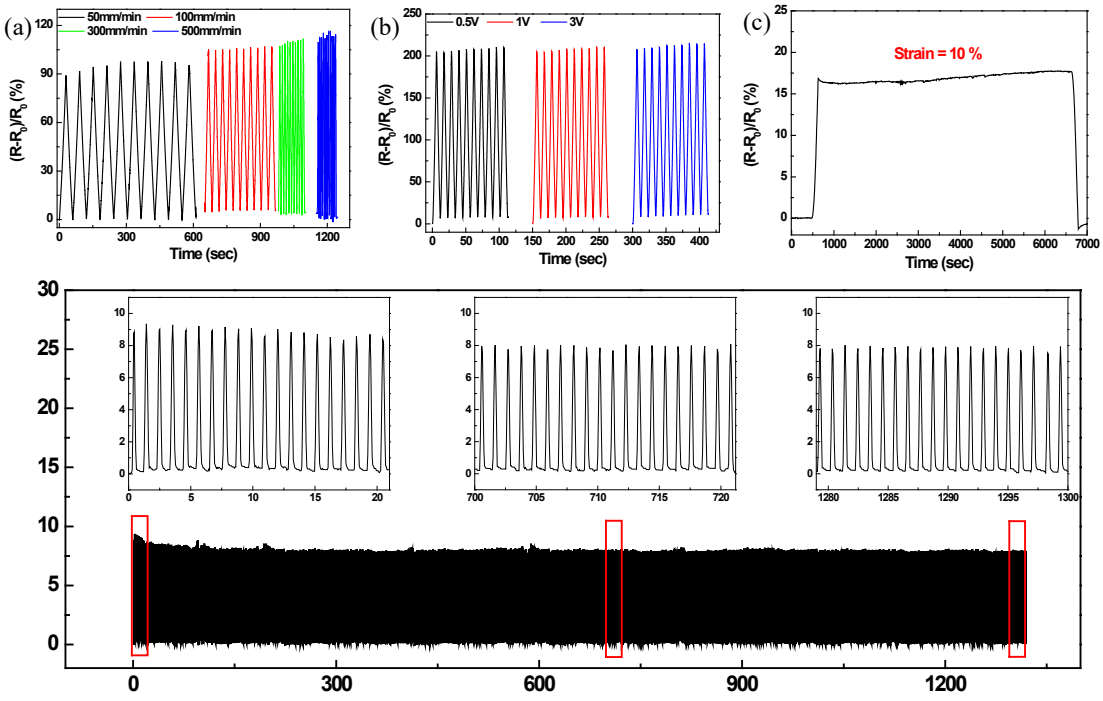

Figure 4. Cyclic stability tests of hydrogel sensor with (a) different stretching rates and (b) different working voltages. (c) Drift characteristics of the hydrogel under a constant strain of 10% for 100 min. (d) Durability test of DN hydrogel sensor for 1300 loading-unloading cycles (The inserted figures show the response signals of cycles 1- 20, 700-720, and 1280-1300, respectively. The response value remains steadily constant, showing the excellent stability of the sensor).

2.3. Applications of flexible strain sensor in monitoring human motions

Considering their many advantages as mentioned above, including unique flexibility, excellent sensitivity and repeatability, wide working range (i.e., stretching rate and working voltage), excellent durability and fast response time, the DN hydrogels may have a wide range of applications in wearable sensing devices for real-time

monitoring of human movement. **Figure 5** presents the applications of hydrogel sensors in detecting the motions of different joints of the human body. Figure 5(a) illustrates the response value to the bending motions of the finger. As the bending degree increased from 0° to 30°, 60°, and 90°, the $\Delta R/R_0$ rapidly increased to a corresponding value of 10%, 23%, 39%, respectively. A certain fixed bending angle of the index finger is associated with a specific $\Delta R/R_0$ value, thanks to the high strain sensitivity and stability of the hydrogel sensor. Similarly, Figure 5(b), 5(c) and 5(d) show the sensing performance of the hydrogel attached to the wrist, elbows and knees, respectively. In all the scenarios, the response value increases along with the bending degree; then the resistance recovers to the original state immediately when the joint is straightened and relaxed. It is worth noting that there are some small peaks in the response signal in Figure 5(d). This is caused by the slight vibration during the bending of the knee, which again demonstrates the excellent strain sensitivity and ultra-fast response of the hydrogel sensors. In addition, as illustrated in Figure 5(e), the sensing performances of the hydrogel sensor were observed when the index finger singly-clicked and doubly-clicked on its surface, respectively. When the hydrogel was pressed, the ion concentration per unit length in the hydrogel system increases, leading to a high sensing signal. Meanwhile, the peak of the sensing signal was consistent with the tapping of the finger. Moreover, placing the hydrogel sensor on different parts of the foot, i.e., tiptoe, sole and heel, the responses of the sensor were recorded when the human body was standing (Figure 5(f)). The responses correspond to the pressure on the tiptoe, sole and heel when the human body is standing. Therefore, the DN hydrogel-based wearable

sensors have great application potential in monitoring human activities and detecting personal health.

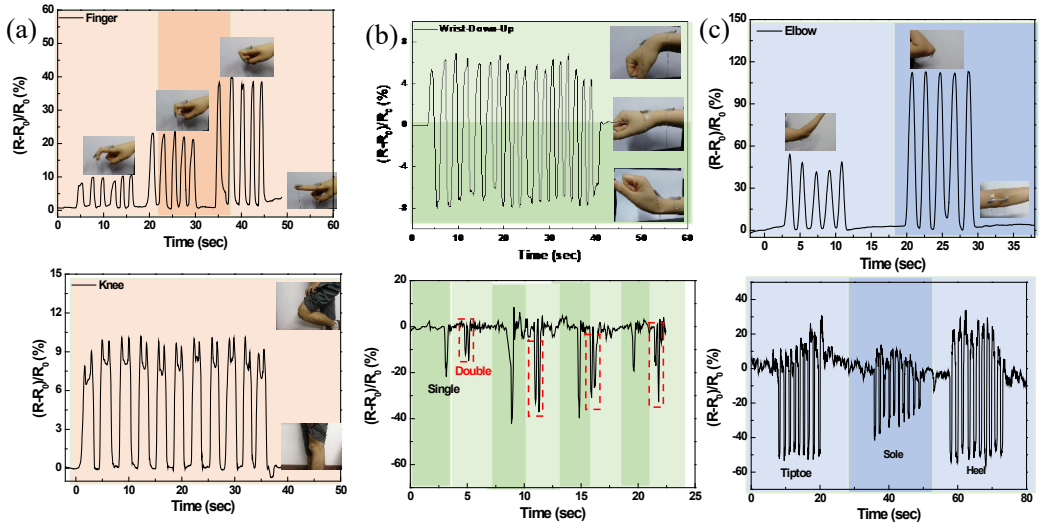

Figure 5. The response of hydrogel strain sensors used to monitor various human movements in real time: (a) The index finger under different bending angles. (b) Bent up and down of wrist. (c) Bent of elbow. (d) Bent of knee joint. (e) The single-click and double-click of the index finger on the surface of sensor. (f) The pressure sensing of the sensor attached to the tiptoe, sole and heel respectively. (The illustrations show the photos of different joints in bending motion).

3. Conclusions

In summary, a high performance PVA/P(AM-AANa) DN ionic hydrogel was prepared based on a simple two-step approach, i.e., free radical in situ polymerizations and freeze-thaw treatment. The obtained DN hydrogel shows high stretchability (549%), high tensile strength (223 KPa) and excellent self-recovery property. Furthermore, the porous network of the hydrogel provides pathways for the transportation of conductive ions (with an excellent conductivity of 25 $mS \cdot cm^{-1}$), resulting in a fast, stable and

reproducible response to different strains. Hence, the prepared hydrogel sensor has high strain sensitivity (a GF of 4.75 to a wide strain of 300%-400%), fast response (360 ms) and excellent sensing stability and reliability. Moreover, the hydrogel sensor can be applied to a variety of different stretching rates (50 mm/min~500 mm/min) and different voltages (0.5 V~3 V). Therefore, it is concluded that the hydrogel can be applied as wearable soft sensors for human motion detecting.

4. Experimental Section

Materials: Acrylamide (AM, 99%), acrylic acid (AA, 99%), polyvinyl alcohol (PVA, average polymerization degree-1700, hydrolysis-99%), potassium persulfate (KPS, 99.99%), sodium chloride (NaCl), N, N′-methylenebisacrylamide (MBAA, 99%), tetramethylethylenediamine (TMEDA, 99%) and sodium hydroxide (NaOH) were supplied by Aladdin. All materials used without further purification. Sodium acrylate (AANa) with a neutralization rate of 90% was obtained through neutralizing acrylic acid with the solution of sodium hydroxide.

Preparation of the hydrogels: A certain amount of PVA (2.375 wt% relative to the weight of the solution) was added to H_2O and the mixture was magnetically stirred at 85 ℃ for 60 min until PVA completely dissolved. Then AM and AANa (3:1 of the molar ratio) were added in the PVA solution and dispersed evenly via magnetic stirring. Subsequently, MBAA and KPS (0.15% and 0.025% of the molar amounts of unsaturated monomers) were added as a crosslinker and an initiator, respectively. The mixture was then stirred to obtain a homogeneous dispersion. TMEDA (0.5%) was

lastly added to the previous solution as an accelerator. After stirring for 30 s to remove the bubbles, the solution was poured into a dumbbell mold and reacted at 30 °C for 12 h to obtain a chemical network cross-linked hydrogel. Then, through the cyclic freeze-thaw treatment, the PVA molecular chains formed the microcrystalline structure and hydrogen bonds, connecting PVA chains with first chemical network to form a double network. Finally, the obtained covalent-microcrystalline DN hydrogel was peeled off from the mold for further tests.

Characterization: Infrared spectra and morphologies of hydrogel samples were respectively identified on a Nicolet IS5 Fourier transform infrared (FT-IR) spectrometer (500 cm^{-1} - 4000 cm^{-1}) and a Zeiss Gemini 500 scanning electron microscope (SEM). The samples for SEM test were firstly freeze-dried and then coated with gold.

Characterization of the hydrogel sensor: The current resistance variations of hydrogel were recorded on an electrochemical workstation CHI810D. The hydrogel samples were prepared in thickness of 2 mm and the electrical conductivity values (σ, $mS \cdot cm^{-1}$) were measured according to the following equation: $\sigma = L/RA$, where L, A and R were respectively the length, cross-sectional area and the electrical resistance of the hydrogel.[24, 47]

For the capability of strain sensing detection, the two ends of hydrogel sensor were sandwiched by conductive wires and fixed on the universal testing machine. It was then connected to the electrodes of the electrochemical workstation through conductive wires. The relative resistance change was defined as the response value of sensor, which was calculated as: $\Delta R/R_0 = (R-R_0)/R_0$, where R and R_0 were the real-time resistance

and the initial resistance, respectively. Then, the sensitivity of the hydrogel-based strain sensor was defined as the gauge factor (GF), GF= $\Delta R/ (R_0*\varepsilon)$. Further, in order to monitor the current signal during motion, the hydrogel sensor (with a thickness of 1 mm, a length of 25 mm, and a width of 10 mm) was respectively attached onto different joints of fingers, wrists, elbows, knees, etc.

Supporting Information

Supporting Information is available from the Wiley Online Library or from the author.

Acknowledgements

This work was supported by the National Natural Science Foundation of China (NO. 52073066), the GDAS' Project of Science and Technology Development (NO. 2020GDASYL-20200102028, NO. 2021GDASYL-20210103094), Science and Technology program of Guangdong Province (NO. 2017B030314137, NO. 2020B0101340005).

Conflict of Interest

The authors declare no conflict of interest.

Reference

[1]Bi S, Hou L, Dong W, Lu Y. *ACS Appl. Mater. Interfaces* **2021**, 13, 2100-2109.

[2]Zhang H, Han W, Xu K, Lin H, Lu Y, Liu H, Li R, Du Y, Nie Z, Xu F, Miao L, Zhu J, Huang W. *Adv. Funct. Mater.* **2021**, 31, 2009466.

[3]Zeng W, Tao XM, Lin S, Lee C, Shi D, Lam K, Huang B, Wang Q, Zhao Y. *Nano Energy* **2018**, 54, 163-174.

[4]Ma M, Shang Y, Shen H, Li W, Wang Q. *Chem. Eng. J.* **2021**, 420, 129865.

[5]Kong H, Song Z, Xu J, Qu D, Bao Y, Wang W, Wang Z, Zhang Y, Ma Y, Han D, Niu L. *Adv. Mater. Technol.* **2020**, 5, 2000677.

[6]Zeng W, Shu L, Li Q, Chen S, Wang F, Tao XM. *Adv. Mater.* **2014**, 26, 5310-5336.

[7]Wang XM, Tao LQ, Yuan M, Wang ZP, Yu J, Xie D, Luo F, Chen X, Wong C. *Nat. Commun.* **2021**, 12, 1776.

[8]Xiang Y, Fang L, Wu F, Zhang S, Ruan H, Luo H, Zhang H, Li W, Long X, Hu B, Zhou M. *Adv. Mater. Technol.* **2021**, 6, 2001157.

[9]Ajeev A, Javaregowda BH, Ali A, Modak M, Patil S, Khatua S, Ramadoss M, Kothavade PA, Arulraj AK. *Adv. Mater. Technol.* **2020**, 5, 2000690.

[10]Liu H, Chen X, Zheng Y, Zhang D, Zhao Y, Wang C, Pan C, Liu C, Shen C. *Adv. Funct. Mater.* **2021**, 31, 2008006.

[11]Zheng Y, Yin R, Zhao Y, Liu H, Zhang D, Shi X, Zhang B, Liu C, Shen C. *Chemical Engineering Journal* **2021**, 420, 127720.

[12]Li Q, Yin R, Zhang D, Liu H, Chen X, Zheng Y, Guo Z, Liu C, Shen C. *Journal of Materials Chemistry A* **2020**, 8, 21131-21141.

[13]Bu Y, Shen T, Yang W, Yang S, Zhao Y, Liu H, Zheng Y, Liu C, Shen C. *Science Bulletin* **2021**. DOI: 10.1016/j.scib.2021.04.041.

[14]Zheng Z, Zhao Y, Hu J, Wang H. *ACS Appl. Mater. Interfaces* **2020**, 12, 47854-47864.

[15]Shi W, Han G, Chang Y, Song H, Hou W, Chen Q. *ACS Appl. Mater. Interfaces* **2020**, 12, 45373-45382.

[16]Yang C, Yin J, Chen Z, Du H, Tian M, Zhang M, Zheng J, Ding L, Zhang P, Zhang X, Deng K. *Macromol. Mater. Eng.* **2020**, 305, 2000479.

[17]Wang Z, Chen J, Cong Y, Zhang H, Xu T, Nie L, Fu J. *Chem. Mater.* **2018**, 30, 8062-8069.

[18]Sun H, Zhao Y, Wang C, Zhou K, Yan C, Zheng G, Huang J, Dai K, Liu C, Shen C. *Nano Energy* **2020**, 76, 105035.

[19]Pu J, Zhao X, Zha X, Li W, Ke K, Bao R, Liu Z, Yang M, Yang W. *Nano Energy* **2020**, 74, 104814.

[20]Liu GS, Yang F, Xu J, Kong Y, Zheng H, Chen L, Chen Y, Wu MX, Yang BR, Luo Y, Chen Z. *ACS Appl. Mater. Interfaces* **2020**, 12, 47729-47738.

[21]Akhtar I, Chang SH. *Adv. Mater. Technol.* **2020**, 5, 2000229.

[22]Hsiao L, Jing L, Li K, Yang H, Li Y, Chen P. *Carbon* **2020**, 161, 784-793.

[23]Zhang Y, Guo M, Zhang Y, Tang C, Jiang C, Dong Y, Law W, Du F. *Polym. Testi.* **2020**, 81, 106213.

[24]Sun X, Qin Z, Ye L, Zhang H, Yu Q, Wu X, Li J, Yao F. *Chem. Eng. J.* **2020**, 382, 122832.

[25]Liu YJ, Cao WT, Ma MG, Wan P. *ACS Appl. Mater. Interfaces* **2017**, 9, 25559-25570.

[26]Qin H, Chen Y, Huang J, Wei Q. *Macromol. Mater. Eng.* **2021**, 2100159.

[27]Dautta M, Alshetaiwi M, Escobar J, Tseng P. *Biosens. Bioelectron.* **2020**, 151, 112004.

[28]Xu J, Wang Z, You J, Li X, Li M, Wu X, Li C. *Chem. Eng. J.* **2020**, 392, 123788.

[29]Li T, Wang Y, Li S, Liu X, Sun J. *Adv. Mater.* **2020**, 32, 2002706.

[30]Song J, Chen S, Sun L, Guo Y, Zhang L, Wang S, Xuan H, Guan Q, You Z. *Adv. Mater.* **2020**, 32, 1906994.

[31]Hang C, Zhao X, Xi S, Shang Y, Yuan K, Yang F, Wang Q, Wang J, Zhang D, Lu H. *Nano Energy* **2020**, 76, 105064.

[32]Hou W, Sheng N, Zhang X, Luan Z, Qi P, Lin M, Tan Y, Xia Y, Li Y, Sui K. *Carbohyd. Polym.* **2019**, 211, 322-328.

[33]Zhu T, Cheng Y, Cao C, Mao J, Li L, Huang J, Gao S, Dong X, Chen Z, Lai Y. *Chem. Eng. J.* **2020**, 385, 123912.

[34]Gan S, Xu B, Zhang X, Zhao J, Rong J. *Int J Biol Macromol* **2019**, 137, 495-503.

[35]Jiao C, Zhang J, Liu T, Peng X, Wang H. *ACS Appl. Mater. Interfaces* **2020**, 12, 44205-44214.

[36]Ge G, Zhang Y, Shao J, Wang W, Si W, Huang W, Dong X. *Adv. Funct. Mater.* **2018**, 28, 1802576.

[37]Wang P, Pei D, Wang Z, Li M, Ma X, You J, Li C. *Chem. Eng. J.* **2020**, 398, 125540.

[38]Gu J, Huang J, Chen G, Hou L, Zhang J, Zhang X, Yang X, Guan L, Jiang X, Liu H. *ACS Appl. Mater. Interfaces* **2020**, 12, 40815-40827.

[39]Cheng B, Chang S, Li H, Li Y, Shen W, Shang Y, Cao A. *Macromol. Mater. Eng.* **2020**, 305, 1900813.

[40]Chen YN, Peng L, Liu T, Wang Y, Shi S, Wang H. *ACS Appl. Mater. Interfaces* **2016**, 8, 27199-27206.

[41]Zhao M, Tang Z, Zhang X, Li Z, Xiao H, Zhang M, Liu K, Ni Y, Huang L, Chen L, Wu H. *Compo. Sci. Technol.* **2020**, 198, 108294.

[42]Pang J, Wang L, Xu Y, Wu M, Wang M, Liu Y, Yu S, Li L. *Carbohyd. Polym.* **2020**, 240, 116360.

[43]Liu S, Li L. *ACS Appl. Mater. Interfaces* **2017**, 9, 26429-26437.

[44]Cai G, Wang J, Qian K, Chen J, Li S, Lee PS. *Adv. Sci.* **2017**, 4, 1600190.

[45]Tian K, Bae J, Bakarich SE, Yang C, Gately RD, Spinks GM, In Het Panhuis M, Suo Z, Vlassak JJ. *Adv. Mater.* **2017**, 29, 1604827.

[46]Jing X, Mi H, Peng X, Turng L. *Carbon* **2018**, 136, 63-72.

[47]Zhang X, Cai J, Liu W, Liu W, Qiu X. *Polymer* **2020**, 188, 122147.